THE JOURNAL OF PHYSICAL CHEMISTRY B
A JOURNAL OF THE AMERICAN CHEMICAL SOCIETY

pubs.acs.org/JPCB

Article

Capturing Hydrated Vanadium Ion Dynamics in Ionomer Nanocomposites Used for Redox Flow Batteries

Xueting Wang, Apoorv Balwani, Madhusudan Tyagi, and Eric M. Davis*

Cite This: *J. Phys. Chem. B* 2024, 128, 5766−5780

Read Online

ACCESS | Metrics & More | Article Recommendations | Supporting Information

ABSTRACT: Herein, we employed high-flux backscattering spectroscopy to capture for the first time the motions of hydrated vanadyl ions in ionomer nanocomposites prepared by both solution-cast and *in situ* sol−gel condensation methods. Both local and jump diffusion coefficients of the hydrated vanadyl (VO^{2+}) ions as well as the dynamic length scales of ion motions and the fraction of immobile hydrogen atoms were extracted from the scattering spectra. Notably, for solution-cast membranes, the jump and local diffusion coefficients of hydrated VO^{2+} ions were seen to decrease by over 10- and 4-fold, respectively, with the introduction of 10 mass % silica nanoparticles (SiNPs) compared to their neat counterparts. Further, the VO^{2+} diffusion coefficients were observed to decrease with thermal annealing, though the impact of annealing was less significant than that seen with the introduction of SiNPs. Finally, in general, thermal annealing and the introduction of SiNPs had no measurable impact on the fraction of immobile hydrogen atoms in both solution-cast and sol-gel ionomer nanocomposites. The data observed in this work, in conjunction with previous structural and chain dynamics studies on hydrated Nafion-SiNP nanocomposites, suggest that a combination of stiffening of the segmental dynamics as well as a decrease in available sulfonic acid groups facilitating transport leads to an overall decrease in mobility of vanadium ions in these ionomer nanocomposites.

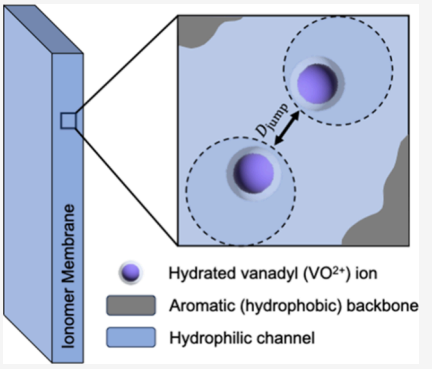

1. INTRODUCTION

With energy obtained from renewable sources becoming more prevalent, scalable energy storage technologies are needed to ensure the reliable dispatch of this energy to the electrical grid. Vanadium redox flow batteries (VRFBs) are a promising energy storage technology due to their quick response time, longevity, flexible design, and relatively low maintenance.[1−3] One critical component of the VRFB is the proton exchange membrane (PEM), which functions to facilitate proton transport while preventing cross-mixing of the positive and negative electrolytes.[4] To address the issue of vanadium ion crossover, researchers have taken a wide variety of approaches, including fabricating layered and sandwiched-structured membranes,[5,6] incorporation of a second polymer phase (i.e., polymer fillers),[7−9] and introduction of inorganic nanoparticles.[10−12] Of these various approaches, the vast majority of the effort has been focused on reducing crossover via the incorporation of inorganic nanoparticles (e.g., silica nanoparticles (SiNPs)). One such class of membranes, sulfonic acid−based ionomer nanocomposites, has garnered considerable attention as PEMs for VRFBs due to their adequate chemical resistance and improved proton selectivity (i.e., the ratio of proton conductivity to vanadium ion permeability).

The current benchmark sulfonated ionomer, Nafion, a perfluorosulfonic acid polymer that has a hydrophobic, poly(tetrafluoroethylene)-based backbone with fluoroether side chains terminated with sulfonic acid groups, has been thoroughly investigated as the PEM for VRFBs. When hydrated, the ionomer forms a nanophase segregated morphology, with the backbone forming hydrophobic domains, while sulfonic-acid-terminated side chains coalesce to form percolated hydrophilic domains that provide a continuous pathway for facile ion transport. To date, researchers have successfully fabricated Nafion−SiNP membranes that exhibit decreased vanadium ion crossover while maintaining similar (though typically reduced) proton conductivities to that of pristine (neat) Nafion.[13,14] Nafion-SiNP nanocomposites are commonly fabricated via two methods: an *in situ* sol−gel condensation process and a solution casting process. In the former, *in situ* growth of the silica phase within the preformed, hydrated perfluorosulfonic acid membrane is achieved via an acid-catalyzed sol−gel reaction involving tetraethoxysilane.[15−17]

More recently, the latter method has been leveraged to prepare ionomer nanocomposites, where preformed, discrete silica nanoparticles are dispersed in an ionomer solution, cast

Received: February 23, 2024
Revised: May 4, 2024
Accepted: May 20, 2024
Published: June 3, 2024

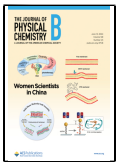

onto a dish, and left to form dense, free-standing membranes (following solvent evaporation).[18] Ionomer nanocomposites fabricated via these two synthesis routes exhibit different nanophase-segregated morphologies, as captured using various small-angle scattering techniques,[15,18,19] which directly impacts the ion transport properties of these membranes.[20] Further, it is known that the silica phase formed by the sol−gel approach is different than that of the discrete SiNPs used for solution-cast Nafion nanocomposites.[12] Along with these two fabrication methods, thermal annealing has also been shown to affect the nanostructure and transport properties of the Nafion membranes.[21,22] In one recent investigation, thermal annealing of Nafion-SiNP nanocomposites (at 140 °C for 2 h) led to a markedly decreased permeability of vanadium ions across the membrane as compared to its unannealed Nafion-SiNP counterpart ($(1.08 \pm 0.12) \times 10^{-8}$ cm^2 s^{-1} vs $(4.45 \pm 0.16) \times 10^{-8}$ cm^2 s^{-1}).[20]

In addition to the permeability of vanadium ions through these ionomers, other fundamental transport properties, such as mutual[23,24] and self-diffusion coefficients of both water and various ions in Nafion membranes have been measured. In particular, the self-diffusivity of cations such as Na^+, K^+, Cs^+, Ag^+, Ca^{2+}, and Ba^{2+} have been characterized via radiotracer methods,[25−27] while the dynamics of water (i.e., the self-diffusivity of water) have been characterized via both nuclear magnetic resonance spectrometer (NMR) and quasi-elastic neutron scattering (QENS).[28−32] In particular, QENS is a unique and powerful technique that can be used to interrogate nano- to picosecond molecular dynamics in restricted geometries.[33] As such, there have been a number of investigations on the dynamics of water in Nafion-based membranes using a variety of QENS techniques, including both time-of-flight (TOF) and backscattering (BS) spectroscopy,[31,33−36] though the former is more commonly used as it captures faster motions (i.e., shorter time scales) than 30 ps.[34,37,38] For example, TOF spectroscopy has been employed to investigate water dynamics in Nafion membranes at various hydration levels.[34] From these experiments, the researchers found that the water dynamics in the low-Q regime could be described using continuous diffusion within a confined space, while in the high-Q region, the dynamics were better characterized as random, unconstrained jump diffusion.

Further, QENS has been used to interrogate the various molecular-level water/ion transport mechanisms in Nafion, i.e., Grotthuss hopping vs vehicular diffusion mechanism, where time-resolved spectra were taken during hydration, going from a state of almost dry to fully hydrated.[33] Capturing both water and ion dynamics in ionomer membranes is imperative for the design of better performing PEMs, as ion transport in these materials is a water-facilitated process.[39] That is, ion and water dynamics are highly coupled in these membranes. While these investigations have provided important insight into the mechanisms of water-assisted proton transport in Nafion, they do not provide any insight into the dynamics of the hydrated vanadium ions, which are also present inside the ionomer during VRFB operation. For us to fully understand the ion transport in PEMs used in VRFBs, it is paramount that we directly capture the dynamics of hydrated vanadium ions inside these materials.

Herein, for the first time, high flux backscattering (HFBS) quasi-elastic neutron scattering experiments were performed to capture the dynamics of the hydrated vanadyl (VO^{2+}) ion inside Nafion and Nafion-SiNP nanocomposite membranes. As the faster dynamics of free water molecules are outside of the time-scale window of HFBS (which ranges from 100 ps to 2 ns), the HFBS measurements were only sensitive to the dynamics of (slower) water molecules bound to the vanadium ion.[40] The ionomer nanocomposites were prepared using two different fabrication routes: (i) an *in situ* sol−gel condensation method on preformed membranes and (ii) solution casting of free-standing membranes from a Nafion dispersion containing discrete SiNPs. To interrogate the impact of SiNPs on the vanadium ion dynamics, membranes were prepared with 4 and 10 mass % SiNP as well as pristine (neat) membranes containing no SiNPs. In addition, the impact of thermal treatment (annealing) on vanadium ion motion was also explored. The local and jump diffusion coefficients of the hydrated VO^{2+} ion within each membrane were extracted from the QENS data, along with additional information such as the fraction of immobile hydrogen atoms. This systematic study provides new insight into the impact of the fabrication method and nanoparticle loading on vanadium ion dynamics within these membranes, which serves to help elucidate the connection between the molecular-picosecond-level dynamics of vanadium ions and the salient macroscopic membrane performance properties, e.g., vanadium ion permeability and proton conductivity.

2. EXPERIMENTAL SECTION

2.1. Materials. Nafion D2021 stock dispersion (Nafion perfluorinated resin solution; 20 mass % in mixture of lower aliphatic alcohols and water; equivalent weight = 1100 g of dry polymer per mol of sulfonic acid) and extruded Nafion 117 membranes (thickness ≈180 μm; equivalent weight = 1100 g of dry polymer per mol of sulfonic acid) were purchased from Ion Power Inc. Tetraethyl orthosilicate (TEOS, > 99.0% purity), methanol (HPLC grade, ≥ 99.9% purity), sulfuric acid (95%−98% purity, ACS reagent), ethanol (200 proof, anhydrous), vanadium(IV) oxide sulfate hydrate (97%), and magnesium sulfate (anhydrous) were purchased from Sigma-Aldrich. Silica (SiO_2) nanoparticles (SiNPs) (colloidal silica in methanol; MT-ST grade; D_P = (10 to 15) nm, where D_P is the particle diameter) were obtained from Nissan Nanomaterials. Hydrogen peroxide (30 mass % in H_2O) was procured from VWR Analytical. Additionally, reverse osmosis (RO) water (resistivity ≈18 MΩ cm) was used for all experiments and membrane synthesis.

2.2. Sample Preparation. *2.2.1. Fabrication of Nafion-SiO_2 Nanocomposite Membranes via an In Situ Sol−Gel Method.* Sol−gel Nafion-SiNP nanocomposite membranes were prepared as previously described.[12] Prior to nanocomposite fabrication, the commercially produced Nafion 117 membranes were subjected to a purification and protonation process, where the ionomer membranes were refluxed for 1 h in each of the following: (1) 3 mass % hydrogen peroxide, (2) followed by deionized water, (3) followed by 0.5 mol L^{-1} sulfuric acid, and (4) finally, deionized water again. After the peroxide and acid steps, the membranes were thoroughly washed with deionized water. Following this procedure, the purified films were dried at 90 °C, under dynamic vacuum, for 24 h to obtain the mass of the dry ionomer membrane. Next, the dried Nafion 117 membranes were equilibrated in a 2:1 (v/v) methanol−water solution for 4 h at room temperature. Following equilibration, a 1.5:1 (v/v) TEOS-methanol solution was added to a stoppered flask containing the equilibrated films as well as 50 mL of the

https://doi.org/10.1021/acs.jpcb.4c01203
J. Phys. Chem. B 2024, 128, 5766−5780

methanol−water solution in which the films were equilibrated. The quantity of TEOS-methanol solution introduced in the flask was determined as to maintain a water to TEOS molar ratio of 4:1. Immediately after the addition of TEOS, the flask was sealed, and the membranes were soaked for the desired residence times (i.e., the time the films were left to soak in the precursor solution). Once removed from the reaction flasks, the films were washed with pure methanol and patted dry to prevent gelation on the surface. Next, the ionomer membranes were dried at room temperature for 24 h followed by thermal annealing for 2 h at 140 °C, after which the oven was turned off and allowed to cool to room temperature. Note that the entire process (from drying to annealing to cooling) was performed under dynamic vacuum. The mass percent of nanoparticles in each membrane was obtained by weighing dry membranes before and after the sol−gel condensation process.

2.2.2. Fabrication of Nafion-SiO_2 Nanocomposite Membranes via Solution Casting. Solution-cast Nafion-SiO_2 nanocomposite membranes were prepared as previously described.[10] Briefly, a dispersion of SiO_2 nanoparticles and Nafion was created by adding a specified amount of the silica nanoparticle solution to the as-received Nafion dispersion. The silica nanoparticle-Nafion mixture was sonicated at least 50 min prior to casting to ensure uniform dispersion of the nanoparticles in the Nafion-SiO_2 dispersion. The Nafion-SiO_2 dispersion was then cast onto a polytetrafluoroethylene (PTFE) substrate and then covered by a funnel with Kim-wipe flue to allow solvent evaporation overnight. Next, the membranes were subjected to the same thermal treatment (annealing) process as the sol−gel membranes, where they were heated 2 h at 140 °C, after which the oven was allowed to cool to room temperature. The entire process (from annealing to cooling) was performed under dynamic vacuum. The mass percent of nanoparticle in membranes was controlled by the amount of SiNP suspension added to the Nafion dispersion.

2.3. Quasi-elastic Neutron Scattering (QENS) − High-Flux Backscattering Spectroscopy. QENS spectra were collectured using the high-flux backscattering spectrometer (HFBS) at the National Institute of Standards and Technology (NIST) Center for Neutron Research (NCNR). Membranes were prepared with the geometry of 8 × 4 cm and a thickness of ≈100 μm, which allowed for ≈90% neutron transmission through the sample. The HFBS experiment was conducted with an energy range of ±17 μeV (resolution of 0.8 μeV) and over a Q-range of 0.25 to 1.6 $Å^{-1}$. To determine the relevant temperatures for the HFBS experiments, fixed window scans (FWSs) for both sol−gel and solution-cast membranes (over a temperature range of 4 to 300 K) were performed. Based on these measurements, 4, 215, 245, and 295 K were selected as the experimental temperatures for both sol−gel and solution-cast Nafion nanocomposite membranes. To best replicate typical vanadium redox flow battery conditions, all the samples were soaked in a 1.5 mol L^{-1} vanadyl sulfate in 3.0 mol L^{-1} sulfuric acid aqueous solution for a period of 48 h. Prior to the beginning of HFBS experiments, the membranes were removed from the acid solution, patted dry, and mounted in the sample cell.

2.4. HFBS Data Analysis. The measured dynamic structure factor $S(Q, \omega)$, where Q and ω are defined as momentum transfer and energy transfer, respectively, can be modeled using the following equation

$$S(Q, \omega) = [A(Q)\delta(\omega) + \{(1 - A(Q))L(Q, \omega)\}] \otimes R(Q, \omega) \quad (1)$$

where $A(Q)$ is the elastic incoherent structure factor ($EISF$), $\delta(\omega)$ is the Dirac delta function, $L(Q, \omega)$ is the Lorentzian function, and $R(Q, \omega)$ represents the instrument resolution function. Herein, the collected scattering data were analyzed by using a model that combines local diffusion within a sphere and random jump diffusion, where the length scale of the confined dynamics was characterized by fitting the $EISF$ for each membrane. The $EISF$ is defined as the ratio of the integrated intensity of the elastic peak to the total integrated intensity (i.e., elastic and quasi-elastic scattering). First, the measured neutron scattering function, $S(Q, \omega)$, was fit with a single Delta function and a single Lorentzian function, which describe the elastic and quasi-elastic component of the scattering, respectively, providing the $EISF$ of samples at different Q values. The Q dependence of $EISF$ can be modeled to extract the parameters representing the geometry of confined motion. The spatial distribution of the moving hydrogen atoms (in our case, hydrogen atoms from water molecules bound to the VO^{2+} ion) was characterized via fitting the $EISF$ to the following equation[40]

$$A(Q) = EISF(Q) = \varphi + (1 - \varphi)\left[\frac{3J_1(QR)}{QR}\right]^2 \quad (2)$$

where φ is the fraction of hydrogen atoms that are not diffusing within the time window of the experiment (i.e., immobile hydrogen ions), R is the radius of the sphere within which the dynamics occur, and $J_1(QR)$ is the first-order Bessel function given by equation below

$$J_1(QR) = \frac{\sin(QR)}{(QR)^2} - \frac{\cos(QR)}{(QR)} \quad (3)$$

Along with the geometric information provided from analysis of the $EISF$ of each membrane, dynamic information on the motions was obtained from the half-width at half-maximum (HWHM, $\Gamma(\mu eV)$) of the Lorentzian function describing quasi-elastic broadening. The HWHM (Γ) has been analyzed using a model developed by Volino et al.,[35,41] where molecular motions are divided into two regimes: (i) one at higher Q values, where standard jump diffusion behavior can be observed and (ii) one at lower Q values, where a plateau in the data appears, providing information about local motions. To extract the mean square jump length, $\langle r^2 \rangle$, and the residence time between jumps (τ), the HWHM were fit with the following equation

$$\Gamma(\mu eV) = \frac{\hbar}{\tau}\left[1 - \exp\left(\frac{-Q^2\langle r^2 \rangle}{6}\right)\right] \quad (4)$$

where $\hbar = 6.582 \times 10^{-16}$ eV s. Using this information, the jump diffusion behavior was obtained via the following equation

$$D_{jump} = \frac{\langle r^2 \rangle}{6\tau} \quad (5)$$

where D_{jump} is the jump diffusion coefficient of hydrated vanadium ions. The confined, local motions of hydrated vanadium ions were obtained via the following equations

https://doi.org/10.1021/acs.jpcb.4c01203
J. Phys. Chem. B 2024, 128, 5766−5780

$$\Gamma_{Q_0} = 4.33\frac{D_{local}}{R^2} \quad (6)$$

$$\Gamma_{Q_0} = \frac{1}{\tau_0} \quad (7)$$

where D_{local} is the local diffusion coefficient and τ_0 is the local residence time.

3. RESULT AND DISCUSSION

Table 1 contains a summary of the various membranes as well as the nomenclature that will be used for said membranes moving forward in the manuscript. As mentioned earlier, Nafion−SiNP membranes were prepared via both *in situ* sol−gel and solution-cast methods. Note that, as seen in Table 1, only thermally treated (or annealed) solution-cast membranes were investigated as unannealed solution-cast membranes would readily redissolve when the membrane was placed in water.

Table 1. Nomenclature for Nafion and Nafion Nanocomposites Containing SiNP Fabricated by Different Methods

fabrication method	thermal treatment	SiNP loading	nomenclature
[-]	[-]	[g SiNP/g Nafion]	[-]
in situ sol−gel	unannealed	0 mass %	Nafion-UA
	annealed	0 mass %	Nafion-A
	annealed	4 mass %	4%SiNP
	annealed	10 mass %	10%SiNP
solution casting	annealed	0 mass %	Nafion-SC
	annealed	4 mass %	4%SiNP-SC
	annealed	10 mass %	10%SiNP-SC

Prior to investigating the dynamics of hydrated vanadium ions, fixed window scans (FWS's) were conducted with the HFBS spectrometer in the "fixed window mode", where the elastic incoherent scattering intensity was measured as a function of temperature. The fixed window scans of sol−gel and solution-cast nanocomposite membranes are shown in Figure S1a,b, respectively. From this analysis, the mean-square displacement (MSD; $\langle u^2 \rangle$) was obtained as $\langle u^2 \rangle$ provides an estimate of the onset of motions and thus, helps provide a suitable temperature range over which to perform dynamic measurements.[42−44] The results of this analysis are shown in Figure 1. Specifically, Figure 1 shows the MSD as a function of temperature for both sol−gel (Figure 1a) and solution-cast (Figure 1b) nanocomposite membranes. We remind the readers that the dynamics captured here are from the water molecules bound to the vanadium ions, as the diffusion coefficients observed in this work are much lower than the diffusion coefficient of free water molecules previously reported in Nafion membranes, as seen in Table 2 and later in the text. Therefore, the measured motions in the work can be considered the dynamics of the hydrated vanadium ion. The molecular-level structure of hydrated vanadium ions have been studied recently, where this structure has been observed stable whether the vanadium ion is in an acidic or aqueous solution. For example, researchers found that the vanadium(IV) ion (i.e., the vanadyl ion, VO^{2+}) in aqueous solution has a octahedral structure, where the hydrated vanadyl ion had an octahedral coordination with four equivalent water molecules in the equatorial plane and a one water molecule in the axial position opposite to the vanadyl oxygen.[45,46] This structure of hydrated vanadyl ion was also evidenced under the chemical environment of the VRFB and the hydrated vanadyl structure was found stable in vanadium concentration from 0.1 to 3 mol L^{-1} (in 3 mol L^{-1} sulfuric acid) within the temperature range of 240 to 340 K.[47] This hydrated form of the vanadium ion makes it possible for us to investigate the vanadium ion dynamics in the Nafion nanocomposite membranes by probing the dynamics of water molecules bound on the vanadium ion.

The linear increase of $\langle u^2 \rangle$ at lower temperatures is arising from harmonic oscillations of atoms around a mean position, i.e., vibrational motions.[48] The lowest MSD was observed at the lowest temperature (≈4 K) for all samples, indicating that all of the atoms in the membranes were "frozen" at this low temperature. Therefore, 4 K was selected to obtain a resolution for dynamic measurements in this study. In both Figures 1a,b, the beginning of an upturn in the MSD data can be observed between 175 to 200 K, which can be attributed to the increasing mobility of molecules in the nanocomposites with increasing temperature. Based on the MSD of these membranes, 215, 245, and 295 K were selected as the temperatures of interest for dynamic investigations, where the minimum temperature of 215 K is slightly above the onset of ion motion, and the maximum temperature of 295 K is room temperature, which is traditionally the working temperature of the VRFB. As seen in Figure 1b, the mean square displacement

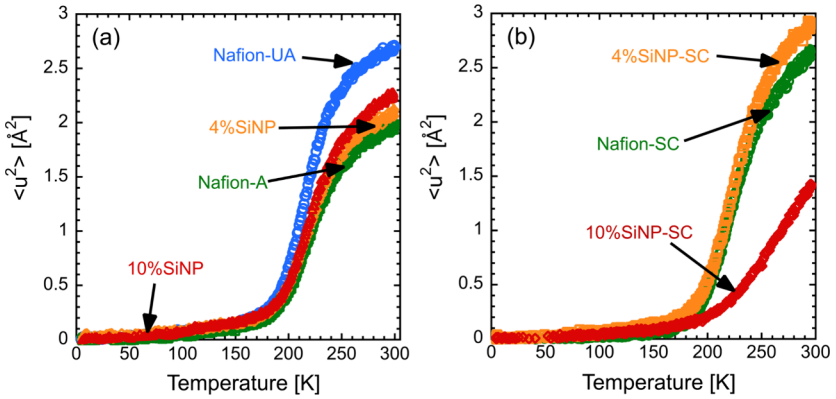

Figure 1. Mean square displacement (MSD; $\langle u^2 \rangle$) for both annealed and unannealed Nafion and Nafion nanocomposite membranes fabricated via (a) *in situ* sol−gel and (b) solution-cast methods.

https://doi.org/10.1021/acs.jpcb.4c01203
J. Phys. Chem. B 2024, 128, 5766−5780

Table 2. Dynamic Parameters of Hydrated Vanadium Ion in This Work (top) and Dynamic Parameters of Water Dynamics in Nafion Reported in Previous Investigations[a]

material	R [$A°$]	φ [-]	Djump [10^{-5} cm^2 s^{-1}]	Dlocal [10^{-6} cm^2 s^{-1}]	τ [ps]	τ_0 [ps]
Nafion-UA	7.28 ± 1.65	0.47 ± 0.040	1.06 ± 0.27	5.12 ± 1.64	41.86 ± 6.26	239.43 ± 4.38
Nafion-A	5.88 ± 0.73	0.51 ± 0.050	0.95 ± 0.31	2.06 ± 0.37	48.43 ± 9.40	388.26 ± 18.40
10%SiNP	6.82 ± 1.10	0.53 ± 0.027	0.50 ± 0.10	4.90 ± 1.11	60.56 ± 6.20	219.15 ± 4.45
Nafion-SC	6.19 ± 1.00	0.40 ± 0.037	0.74 ± 0.26	3.72 ± 0.84	56.78 ± 16.07	237.31 ± 4.43
10%SiNP-SC	5.42 ± 0.71	0.65 ± 0.020	0.06 ± 0.039	0.93 ± 0.18	273.09 ± 67.79	733.52 ± 39.09
Nafion 117 (λ_{water} = 1)	2.10 ± 0.22	0.852 ± 0.010	1.22 ± 0.08	0.38 ± 0.36	14.7 ± 1.1	27.0 ± 15.9
Nafion 117 (λ_{water} = 8)	3.46 ± 0.04	0.169 ± 0.006	1.86 ± 0.08	0.91 ± 0.06	4.4 ± 0.3	11.2 ± 0.5
Nafion 117 (λ_{water}= 16)[34]	3.66 ± 0.03	0.119 ± 0.005	2.14 ± 0.08	1.04 ± 0.12	3.6 ± 0.3	9.8 ± 0.7
Nafion 115[36]	1.92 ± 0.07	0.5	1.4		4.4	8.5
Nafion 112[32]	4.2 ± 0.3		2.0 ± 0.1		2.5 ± 0.4	
bulk water[64,65]			Translational (self) diffusion D_t = 2.36		1.3	

[a]Nafion 117 (λ_{water} = 1), Nafion 117 (λ_{water} = 8), and Nafion 117 (λ_{water} = 16) represent water dynamics in Nafion 117 at various hydration levels (λ_{water}), where Nafion 117 (λ_{water} = 1) is the lowest hydration level and Nafion 117 (λ_{water} = 16) is fully hydrated. Note that the level of hydration, λ_{water}, is the molar ratio of the water and sulfonic acid groups of the Nafion membrane, and the data in the table are the dynamics collected at room temperature.

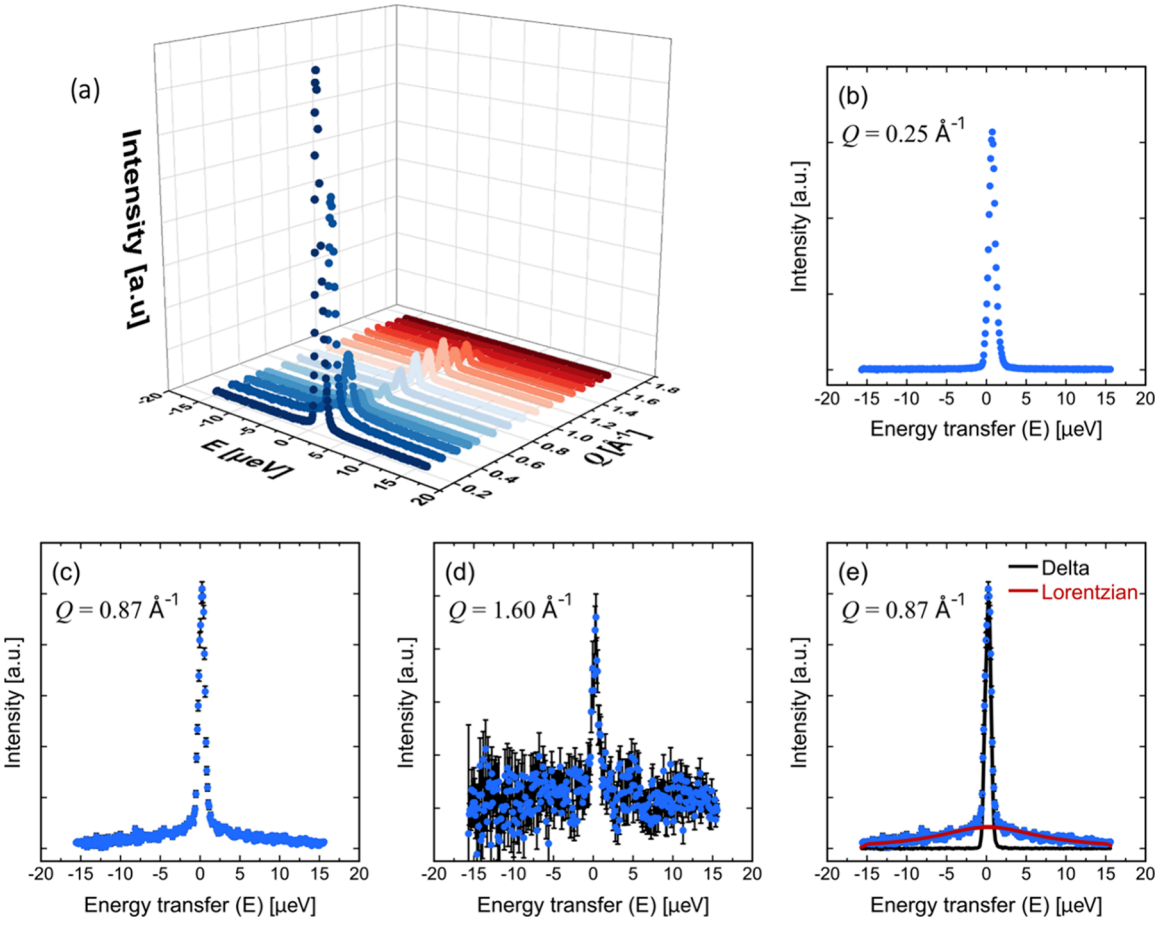

Figure 2. Quasi-elastic neutron scattering (QENS) spectra for Nafion-SC membranes at 295 K and (a) over the entire Q range, (b) at Q = 0.25 Å^{-1}, (c) at Q = 0.87 Å^{-1}, and (d) at Q = 1.60 Å^{-1}. (e) QENS spectra of Nafion-SC at 295 K and at Q = 0.87 Å^{-1}, where the solid black and red lines represent the best-fit Delta (elstic) and Lorentzian (quasi-elastic) functions, respectively.

of 10%SiNP-SC over the temperature range investigated (200 to 300 K) is significantly lower than the other two solution-cast samples, indicating a higher concentration of immobile atoms and slower dynamics in solution-cast Nafion sample containing 10 mass % SiNPs. Reduced dynamics at higher silica concentrations has been previously observed for solution-cast Nafion nanocomposites using neutron spin echo (NSE) spectroscopy, corroborating the retarded dynamics observed with HFBS.[12]

Based on the data shown in Figure 1, quasi-elastic scattering spectra for all membranes were collected at 4, 215, 245, and 295 K, where motions were collected at 16 different Q values, providing spatial information on the observed dynamics. For reference, the QENS spectra for Nafion-SC, collected at 295 K, are shown in Figure 2a, where the energy transfer centers at a

https://doi.org/10.1021/acs.jpcb.4c01203
J. Phys. Chem. B 2024, 128, 5766−5780

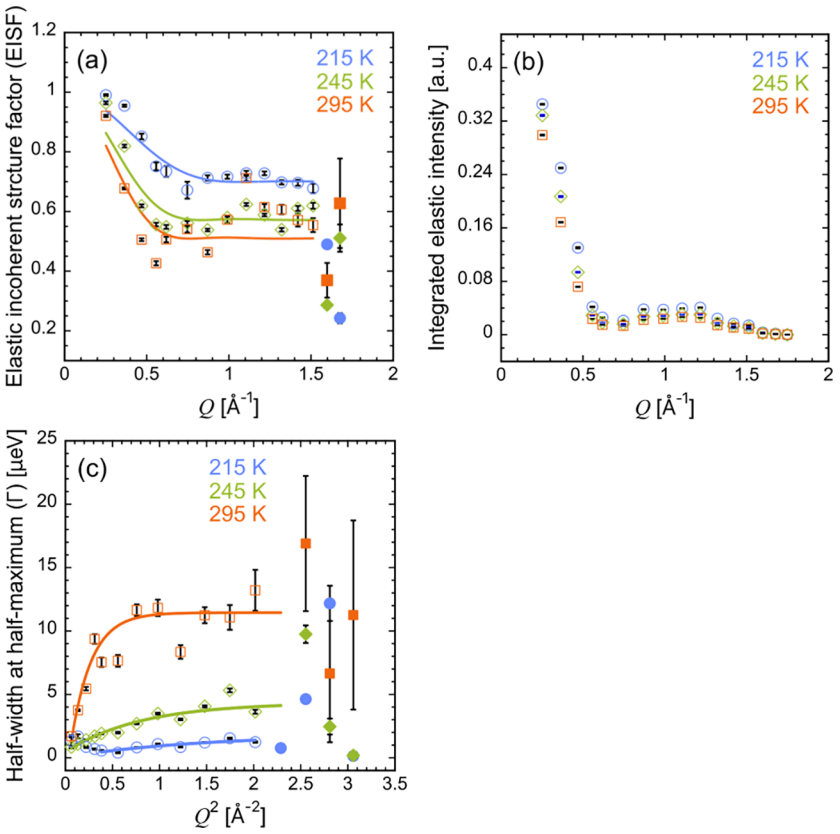

Figure 3. (a) Elastic incoherent structure factor (*EISF*), (b) integrated elastic intensity, and (c) half-width at half-maximum (HWHM) for Nafion-A at 215 (blue circles), 245 (green diamonds), and 295 K (orange squares). The solid lines in (a) and (c) represent the best fit obtained from nonlinear regression. Note that the error bars for the *EISF* and HWHM data result from the fitting of the scattering data using the Delta and Lorentzian functions.

value of 0 μeV for quasi-elastic scattering. To better highlight the diffusional motions observed with HFBS, QENS data collected at low-Q (0.25 Å^{-1}), mid-Q (0.87 Å^{-1}), and high-Q (1.60 Å^{-1}) are also presented in Figure 2b–d. As seen in Figure 2b, the scattering observed in the QENS data appears to be primarily elastic, as the ion motions are undetectable at a length scale, which is significantly larger than the length scale of the ion dynamics. That is, there is little to no quasi-elastic broadening observed in the QENS data. In contrast, at a higher Q value, like that shown in Figure 2c, we begin to observe broadening in the data, which arises from the diffusive behavior of the hydrated vanadium ion. Finally, as seen in Figure 2a,d, the scattering data at high-Q values (e.g., Q = 1.60 Å^{-1}) have large error, as well as low intensity, as the signal from the ion dynamics is convoluted by the instrument noise at such small length scales.

To extract elastic and quasi-elastic information from the QENS data, the scattering data were regressed to both a Delta function (solid black line) and a Lorentzian function (solid red line). An example of this regression at Q = 0.87 Å^{-1} is shown in Figure 2e. The *EISF* values for Nafion-A at 215 (blue circles), 245 (green diamonds), and 295 K (red squares) are shown in Figure 3a, where *EISF* is plotted as a function of the wave vector transfer (Q). Interestingly, a peak in the *EISF* data is observed from 0.8 < Q < 1.5 Å^{-1}, at all temperatures investigated. To better understand the origin of the peak located between 0.8–1.5 Å^{-1} in the *EISF* data, the contribution from elastic scattering was obtained by integrating the area under the Delta function, which is shown far all three temperatures in Figure 3b. As seen in Figure 3b, the same peak that was observed in the *EISF* data is also present in the elastic scattering portion of the total scattering. Therefore, the peak in the *EISF* data can be attributed to the elastic scattering from the sample. This peak has been previously observed in QENS data of Nafion and has been attributed to the elastic coherent scattering from the polymer backbone.[31] This feature, arising from the structural arrangement of the backbone of Nafion, was further investigated, where both dry Nafion membrane, as well as deuterium-exchanged samples were studied to help better parse the elastic contributions from hydrogen in the water (H_2O) and the Nafion backbone.[40] Additionally, as shown in Figure 3a, decreasing *EISF* was observed as temperature increased from 215 to 245 K and to 295 K, which indicates dynamics were more vigorous with higher temperature, leading to less immobile ions for elastic scattering. In addition, a plateau can be observed at higher Q values, which is indicative of immobile atoms on the time scale of the instrument. As can be seen, as temperature increases, more and more atoms take part in the motion modeled by the Lorentzian function.

Geometrical information regarding the motions of the hydrated vanadium ions can be extracted by regressing the *EISF* vs Q data via eq 2, where the radius of the sphere within which dynamics occur (R) and the fraction of immobile hydrogen atoms (φ) were obtained from the regression, which is shown as the solid (colored) lines in Figure 3a. In addition to this geometrical information, the dynamic information on the observed ion motions can be obtained from the half-width

https://doi.org/10.1021/acs.jpcb.4c01203
J. Phys. Chem. B 2024, 128, 5766–5780

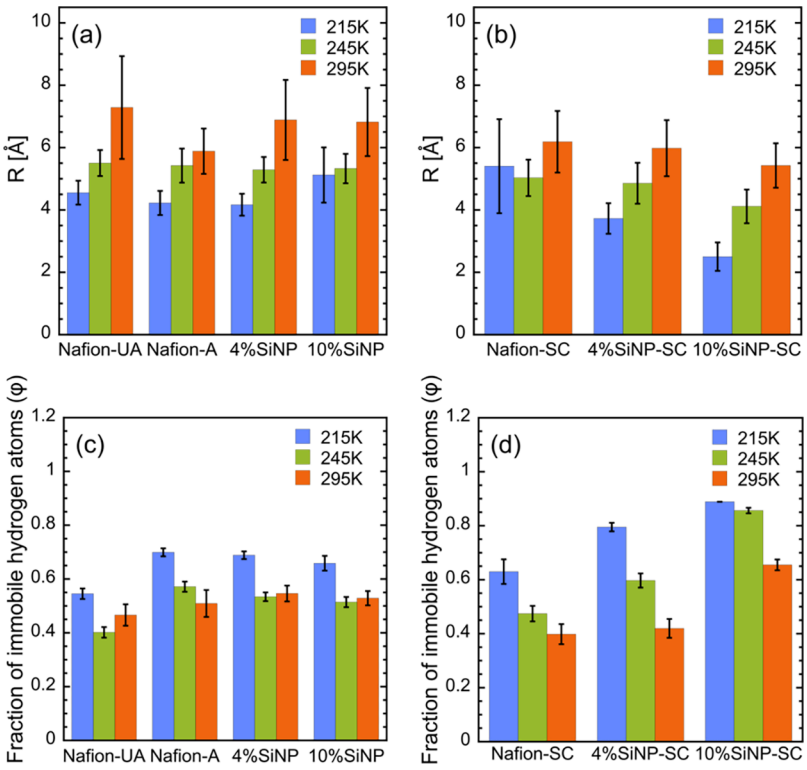

Figure 4. Radius of sphere within which dynamics occur (R) for Nafion and Nafion nanocomposite membranes fabricated via (a) *in situ* sol−gel and (b) solution-cast methods, as well as the fraction of immobile hydrogen atoms (φ) for Nafion and Nafion nanocomposite membranes fabricated via (c) *in situ* sol−gel and (d) solution-cast methods, at 215 K (solid blue bar), 245 K (solid green bar), and 295 K (solid orange bar).

at half-maximum (HWHM) data of the Lorentzian function. The HWHM data for Nafion-A at 215 K (blue circles), 245 K (green diamonds), and 295 K (red squares) vs Q^2 are shown in Figure 3c. In such a representation, Fickian diffusion results in a linear plot slope of which provides values of diffusion coefficient. A plateau at higher Q values is a clear indication of the jump-diffusion process given by eq 4. The HWHM data were regressed to eq 4, where the mean square jump length ($\langle r^2 \rangle$) and the residence time between diffusional jumps (τ) were obtained from the regression. The result of this regression is shown as solid (colored) lines in Figure 3c. Note that *EISF* and HWHM data along with the best fitting from nonlinear regression for all samples are provided in Figures S2 and S3 in the Supporting Information. It should be noted that the HWHM shown in this work is significantly lower than that of captured water dynamics in Nafion membranes in previous studies (∼ 10 μeV vs ∼0.1 meV).[34,36]

Figure 4 shows the results of the *EISF* data regression, where the radius of the sphere within which dynamics occur (R) and the fraction of immobile hydrogen atoms (φ) for Nafion-SiNP nanocomposites fabricated via sol−gel and solution casting are shown in Figure 4a,c and 4b,d, respectively. While discussion here will mainly focus on the ion dynamics at room temperature (295 K), as this is typical operating temperature for VRFBs, in general, the length scale of motions is seen to increase with increasing temperature for both sol−gel and solution-cast samples. As seen in Figure 4a, at room temperature, the impact of thermal treatment has little impact on the value of R, 7.28 ± 1.65 Å for Nafion-UA vs 5.88 ± 0.73 Å for Nafion-A. These data suggest that the significant reduction in vanadium ion permeability that has been observed for annealed membranes (44.0×10^{-9} cm^2 s^{-1} for Nafion-UA vs 11.0×10^{-9} cm^2 s^{-1} for Nafion-A)[20] cannot directly be attributed to changes in the dynamic length scale of vanadium ion self-diffusion. The transport of ions through ionomers, such as Nafion, is directly coupled to polymer morphology (i.e., nanostructure),[52] as well as chain dynamics,[49,50] both of which can be affected by thermal treatment of the membrane. Annealing is usually performed at a temperature higher than the glass transition temperature (T_g), leading to an increased order of the backbone packing. For example, previous work on the segmental and swelling dynamics of Nafion suggested that the ionomer network become stiffer after annealing, which led to a reduction in vanadium ion transport.[12] In addition, decreased mobility of the Nafion backbone with thermal annealing has been previous observed, though interestingly, the highest proton conductivity was observed with membranes annealed at the highest annealing temperature of 140 °C.[21] Therefore, as the markedly decreased vanadium ion permeability cannot solely be attributed to a reduction in the radius of the hydrated vanadium ion dynamics, this reduction is more than likely related to a stiffening and overall decrease in polymer chain flexibility in these annealed ionomer membranes. As seen in Figure 4a, the introduction of silica into the sol−gel membranes does not lead to a measurably different value of R when compared to that of Nafion-A, indicating that introduction of SiNPs in sol−gel membranes does not have notable impact on the length scale of vanadium ion self-diffusion dynamics within the ionomer nanocomposite. Interestingly, previous measurements of vanadium ion permeability on these sol−gel membranes from our group showed that the introduction of silica nanoparticles at higher concentrations did not measurably impact the permeability of vanadium ions through the membranes (11.0×10^{-9} cm^2 s^{-1}

https://doi.org/10.1021/acs.jpcb.4c01203
J. Phys. Chem. B 2024, 128, 5766−5780

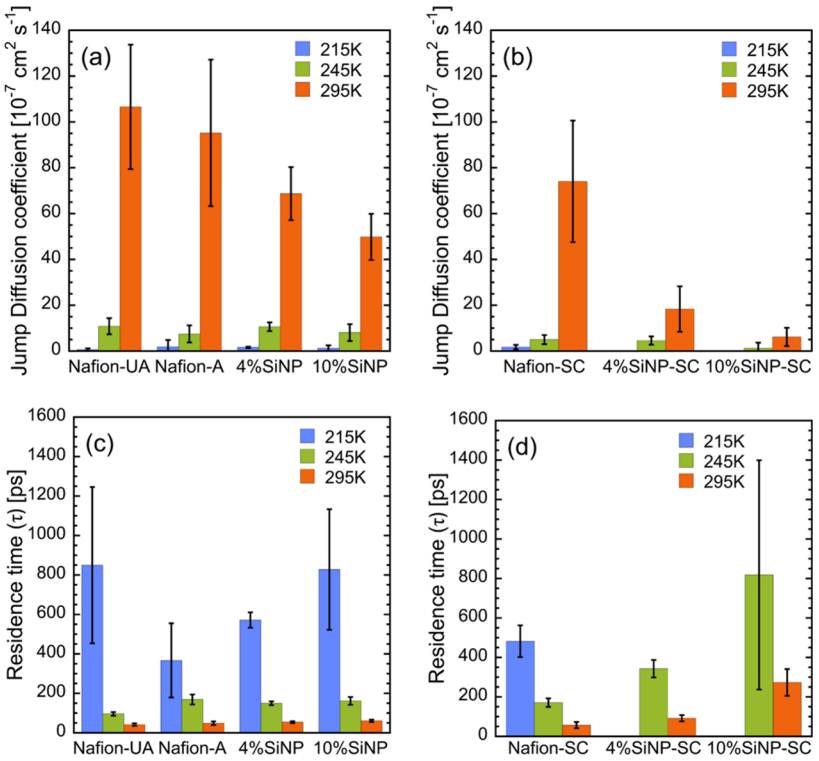

Figure 5. Jump diffusion coefficient (D_{jump}) for Nafion and Nafion nanocomposite membranes fabricated via (a) *in situ* sol−gel and (b) solution-cast methods, as well as the residence time (τ) for Nafion and Nafion nanocomposite membranes fabricated via (c) *in situ* sol−gel and (d) solution-cast methods, at 215 K (solid blue bar), 245 K (solid green bar), and 295 K (solid orange bar).

for Nafion-A vs 10.7×10^{-9} cm^2 s^{-1} for Nafion-10SiNP),[20] which correlates with the similar R values for these membranes.

In contrast, the vanadium ion permeability was seen to decrease in SiNP-Nafion composite membranes fabricated via solution casting (9.0×10^{-9} cm^2 s^{-1} for Nafion-SC vs 5.5×10^{-9} cm^2 s^{-1} for Nafion-5%SiNP-SC),[20] while noticeable changes in the value of R for solution-cast samples at room temperature (295 K) was not observed (6.19 ± 1.00 Å to 5.98 ± 0.90 Å to 5.42 ± 0.7 Å when NP loading is increased from 0 mass % to 4 mass % to 10 mass %, respectively), as shown in Figure 4b.[51] While smaller SiNPs may interact with vanadium ions directly through steric hindrance, these nanoparticles still affect ion transport markedly via stiffening of the polymer network and via interactions of vanadium with the overall negatively charged surface of the unfunctionalized SiNPs. Notably, while the smallest length scale (R) of vanadium ion dynamics at room temperature is 5.42 ± 0.7 Å (for 10%SiNP-SC), it is still larger than that of pure water dynamics in Nafion at room temperature, where a value of 3.66 ± 0.03 Å was obtained from QENS measurements of hydrated Nafion membranes.[34] This is believed to be directly related to the larger size of the hydrated vanadyl ion ($VO^{2+}{\cdot}5H_2O$) when compared to that of water molecules. These results further support the claim that the dynamics being captured in these systems is that of the hydrated vanadium ion, i.e., water bound to the vanadium ion, and not that of simply water. The smaller length scale of pure water dynamics in Nafion has also been observed by other researchers,[36] who found that the value of R occur increased linearly when the temperature was increased from 200 to 260 K, after which it remained at a value of approximately 2 Å until the highest temperature investigated of 300 K was reached. Again, we note that this value is also smaller than the length scale of the vanadium ion dynamics measured here.

Another parameter arising from the *EISF* analysis is the fraction of immobile hydrogen atoms (φ), which is shown in Figures 4c,d for sol−gel and solution-cast nanocomposites, respectively. It should be noted that the fraction of immobile hydrogen atoms discussed here is related to the hydrated vanadium ions, essentially indicating the mobility of vanadium ions in these nanocomposite membranes. Water dynamics in hydrated Nafion membranes has been previously investigated with QENS, where the fraction of immobile hydrogen atoms in fully hydrated Nafion 117 (equivalent to "Nafion-UA" in this work) was 0.119 ± 0.005 at room temperature, which is significantly lower compared with the fraction of immobile hydrogen atoms (or hydrated vanadium ion) measured in this work (0.47 ± 0.0398 for Nafion-UA). As the smaller sized water molecules and hydrated protons (i.e., hydronium ions) have higher mobility, transport of these molecules through the ionomer is less restricted when compared with the hydrated vanadium ion.[34]

As seen in Figure 4c, the value of φ is a function of both thermal annealing and the presence of the silica phase within the ionomer matrix. For example, the fraction of immobile hydrogen atoms is lower for Nafion-UA than for Nafion-A, at all temperatures, indicating how the increase in crystallinity and overall membrane stiffness[52] with annealing also results in a value of φ for these membranes. Notably, after the first reduction in φ when the temperature was increased from 215 to 245 K, the value of φ did not markedly change when temperature was further increased from 245 to 295 K. As seen in Figure 4c, once the temperature reaches 295 K, there is no measurable difference in the value of φ for Nafion-A, 4%SiNP, and 10%SiNP. In contrast, for all solution-cast membranes, the

https://doi.org/10.1021/acs.jpcb.4c01203
J. Phys. Chem. B 2024, 128, 5766−5780

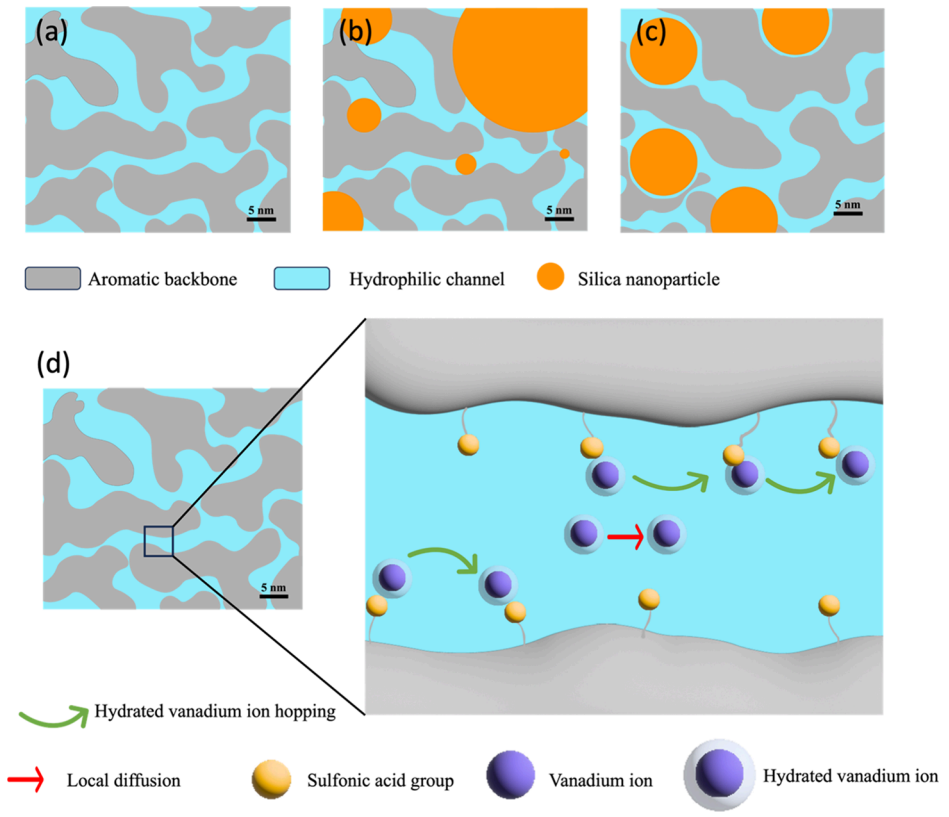

Figure 6. Illustrative schematics of the hydrated nanostructures of (a) neat Nafion, (b) Nafion-SiNP nanocomposites prepared via an *in situ* sol−gel method, and (c) Nafion-SiNP nanocomposites prepared via a solution-cast method. (d) Illustrative schematic of vanadium ion transport through the hydrated, hydrophilic channels of Nafion.

fraction of immobile hydrogen atoms was seen to decrease gradually when the temperature was increased from 215 to 295 K. Further, at room temperature, no measurable difference was observed for the value of φ with the introduction of 4 mass % SiNPs (0.4 ± 0.037 vs 0.42 ± 0.035 for Nafion-SC vs 4%SiNP-SC). However, once the SiNP loading was increased to 10 mass %, significantly constrained motions were observed, where the value of φ was seen to increase to 0.65 ± 0.02 for 10%SiNP-SC, which is an over 50% increase when compared to both Nafion-SC and 4%SiNP-SC. In contrast to the results presented in Figure 4a,b, the introduction of SiNPs was seen to have a greater influence on the concentration of mobile vanadium ions than on the overall length scale of the ion dynamics, a parameter that was seen to be similar at room temperature for solution-cast membranes. When comparing the data in Figure 4c to those in Figure 4d, we observe that the incorporation of SiNPs into sol−gel samples had far less of an effect on the value of φ when compared to simple thermal annealing. This difference in behavior between solution-cast and the *in situ* sol−gel ionomer nanocomposites could be attributed to differences in the hydrated nanostructure of the composite membranes, as well as the differences in "silica density" between the two fabrication routes.[20] Notably, the silica phase for sol−gel fabricated membranes is formed within a preformed Nafon membrane via a condensation reaction, leading to a heterogeneous, less dense silica phase. In contrast, the solution-cast method employs a dispersion/suspension containing the iononmer and preformed, solid SiNPs. Moreover, in this fabrication method, the ionomer chains have significantly higher conformational entropy, giving them the ability to interact with the surface of the SiNPs, and rearrange as the solvent evaporates, forming a dense, free-standing membrane. The schematic nanostructure of neat Nafion, Nafion-SiNP nanocomposite membranes prepared via an *in situ* sol−gel process, and a solution-cast method are shown in Figure 6a−c.

Along with the *EISF* discussion, the half-width at half-maximum (HWHM) was analyzed to provide information regarding the dynamics of the ion motions. As mentioned earlier, the HWHM data are presented in Figure 3c. These data were regressed to eqs 4 and 5 to obtain both the jump diffusion coefficient (D_{jump}) and the residence time (τ). The former can be thought of as the speed at which ions hop from one site to a neighboring site, while the latter can be considered a measure of the time span between jumps. The jump diffusion coefficient for membranes fabricated via *in situ* sol−gel and solution-cast methods, at 215 K (blue), 245 K (green), and 295 K (orange), are shown in Figure 5a,b, respectively. Note that the jump diffusion coefficients for 4%SiNP-SC and 10%SiNP-SC at 215 K are not shown in Figure 5b as the dynamics are too slow at this temperature to be captured by the QENS instrument. We note that at 215 K, the lowest R values (3.7 ± 0.49 and 2.5 ± 0.45 Å) and highest values of φ (0.79 ± 0.016 and 0.89 ± 0.001) were observed for 4%SiNP-SC and 10%SiNP-SC membranes as seen in Figure 4b,d. The large fraction of immobile hydrogen atoms is indicative of less quasi-elastic scattering between the neutrons and bound water molecules, indicating less vigorous dynamics. In addition, the dynamics of hydrated vanadium ions were effectively restricted by the incorporation of SiNPs in solution-cast samples, further leading to weak dynamics for 4%SiNP-SC and 10%SiNP-SC at 215 K.

https://doi.org/10.1021/acs.jpcb.4c01203
J. Phys. Chem. B 2024, 128, 5766−5780

As seen from Figure 5a,b, in general, the values of D_{jump} increased markedly with increasing temperature for all samples. We note that our discussion moving forward will focus on the values of D_{jump} at 295 K, as again, this is the operating temperature of a working redox flow battery. As seen in Figure 5a, Nafion membrane containing no nanoparticles demonstrated reduced jump diffusion coefficient with thermal treatment (Nafion-A) when compared with their unannealed counterpart (Nafion-UA), suggesting that annealing can lead to slower vanadium ion dynamics, which is consistent with the reduced R as well as previously observed reduced vanadium ion permeability for these annealed ionomers. Furthermore, the value of D_{jump} was seen to decrease for both *in situ* sol−gel and solution-cast membranes with both the introduction of SiNPs (Nafion-A vs 4%SiNP and Nafion-SC vs 4%SiNP-SC) as well as with increases in SiNP loading (4%SiNP vs 10%SiNP and 4%SiNP-SC vs 10%SiNP-SC), which again, is in accordance with the reduced vanadium ion permeability via introduction of SiNPs in Nafion previously reported by our group.[20,51] This observed decrease in D_{jump} with the incorporation of silica nanoparticles can be attributed to the interactions between SiNPs and the ionomer network as well as the altered nanostructure of the membrane after the introduction of SiNPs. A recent study on ion transport in the Nafion membrane suggested that silica nanoparticles may adhere to the hydrophilic channel wall and interact with the sulfonic acid groups along the ionic channel, reducing the accessibility of sulfonic groups facilitating vanadium ion transport, leading to decreased vanadium ion crossover.[53,54] It should also be noted that vanadium cations have been shown to bind inside Nafion membrane with a higher preference than protons (H^+) due to their higher affinity to the sulfonic acid groups,[55−57] while stronger electrostatic interaction arising from strong affinity of cations to sulfonic acid site can lead to lower mobility of cations, which further leads to a reduction in the transport of vanadium ions in the ionomer membrane.[58,59]

Details regarding these interactions in Nafion membranes under the chemical environment of vanadium redox flow batteries electrolytes has been previously investigated using a combination of X-ray photoelectron spectroscopy (XPS), nuclear magnetic resonance (NMR) spectroscopy, and ultraviolet visible (UV−vis) spectroscopy.[60] In that study, a four-state model (proposed by Mauritz)[61] was applied to analyze the interactions between hydrated vanadium ions and the sulfonic acid groups of Nafion. Interestingly, they found that hydrated vanadyl ions interact with sulfonic acid groups via the protons on the water molecules in the vanadyl hydration shell rather than direct binding of the vanadium ion, which was further confirmed as peak changes representing formation of contact ion pairs were not observed in both ^{19}F NMR and UV−vis spectra. They noted that as electrostatic attraction between positively charged vanadium ion and negatively charged sulfonic acid groups is shielded by water molecules, providing hydrated vanadium ion some mobility, the nature of these hydrogen bonds further facilitates the dynamics of positively charged hydrated vanadyl ion, where hopping of the vanadium ion between neighboring sulfonic acid sites was achieved with the interaction between cation and sulfonic acid groups.[60,61]

A schematic figure demonstrating this ion hopping transport of the hydrated vanadium ion is shown in Figure 6d. Therefore, we posit that the introduction of SiNPs in both *in situ* sol−gel and solution-cast membranes significantly restricted hopping of hydrated vanadium ions as fewer sulfonic acid groups were available for ion hopping, leading to decreased jump diffusion coefficients, providing a deeper understanding of the origin of reduced vanadium ion permeability from an atomic scale. Similar to hopping of hydrated vanadium ions, proton hopping is one of the mechanisms for proton transport in hydrated ionomer membranes, where protons hop from site to site. As such, the model used in this work (jump diffusion within a sphere) has been applied to understand water dynamics in Nafion membranes with QENS as well, where a value for jump diffusion coefficient from proton hopping at room temperature was reported to be $(2.14 \pm 0.08) \times 10^{-5}$ cm^2 s^{-1},[34] which is notably higher than the hydrated vanadyl ion jump diffusion coefficient in the same membrane measured in this work ($1.06 \pm 0.27) \times 10^{-5}$ cm^2 s^{-1} for "Nafion-UA"). We note that the value of D_{jump} for Nafion-UA was the highest value of D_{jump} observed in this work. We again point out that in this work, the jump diffusion of free protons was not observed, as motions of free protons are significantly faster when compared with that of hydrated vanadyl ion (orders of magnitude lower residence times, τ), and thus, are out of the dynamic window of high flux backscattering. When looking at the combination of the results of the jump diffusion coefficient (D_{jump}), the radius of the dynamics of motions (R), and the fraction of immobile hydrogen atoms (φ), it is evident that motions of the hydrated vanadyl ion are more restricted (i.e., less mobile) compared to free water in Nafion.

In addition to the jump diffusion coefficient, we also extracted the residence time between jumps (τ) from the HWHM analysis. The value of τ for *in situ* sol−gel and solution-cast samples, at 215 K (blue), 245 K (green) and 295 K (orange), are shown in in Figures 5c,d. Analogous to the data for D_{jump}, the residence time between jumps for 4%SiNP-SC and 10%SiNP-SC at 215 K are not showed in Figure 5d as the dynamics were too slow to be captured within the experimental window of HFBS. As expected, for membranes prepared via both fabrication routes, the value of τ decreased significantly with increasing temperature. From Figure 5c, we observe that, at room temperature, the value of τ increased with both the introduction of SiNPs, as well as increased with an increase in SiNP loading (48.93 ± 9.4 ps, 54.03 ± 4.62 ps and, 60.56 ± 6.2 ps, for Nafion-A, 4%SiNP and 10%SiNP, respectively) for *in situ* sol−gel samples, which is coincides with the decreased value of D_{jump} for these membranes, further underscoring the slower vanadium ion dynamics with the introduction of SiNPs into the Nafion membrane. Additionally, we note that larger residence times were also observed for Nafion membranes after thermal treatment (48.93 ± 9.4 ps vs 41.86 ± 6.3 ps for Nafion-A vs Nafion-UA), which is in agreement with the jump diffusion coefficient as higher D_{jump} indicates more vigorous dynamics, and therefore a shorter residence time.

The impact of the SiNPs on the vanadium ion dynamics is even more pronounced for solution-cast membranes, where as seen in Figure 5d, the value of τ, at room temperature, for Nafion-SC, 4%SiNP-SC, and 10%SiNP-SC are 56.78 ± 16.08, 91.88 ± 15.76, and 273.09 ± 67.79 ps respectively. When compared to their sol−gel fabricated counterparts in Figure 5c, we observe that, in general, the value of τ is between approximately 2- to 4-fold longer for solution-cast nanocomposites. These longer residence times for solution-cast

https://doi.org/10.1021/acs.jpcb.4c01203
J. Phys. Chem. B 2024, 128, 5766−5780

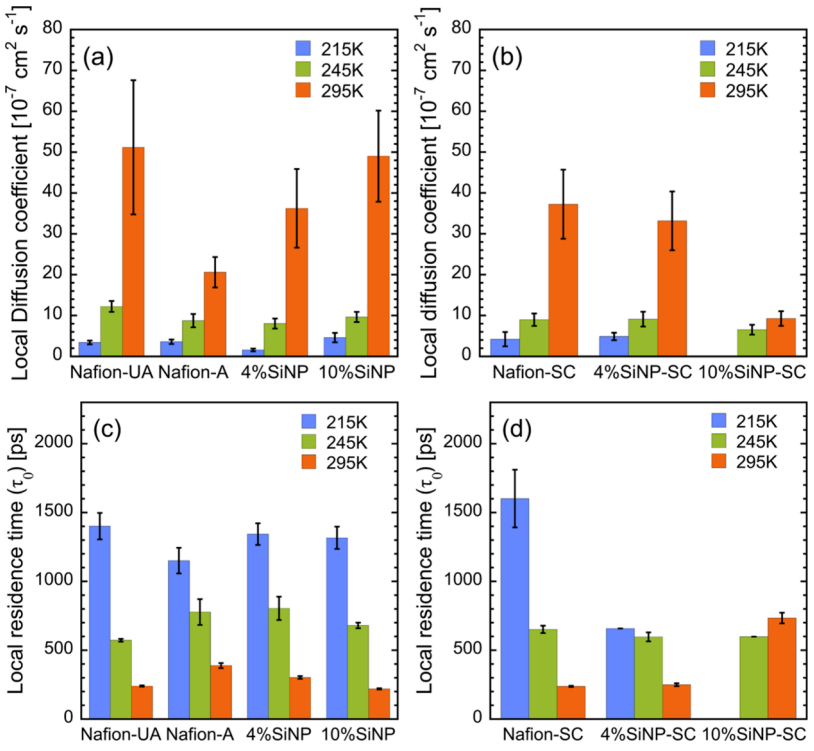

Figure 7. Local diffusion coefficient (D_{local}) for Nafion and Nafion-SiNP nanocomposites fabricated via (a) *in situ* sol−gel and (b) solution-cast methods as well as the local residence time (τ_0) for Nafion and Nafion-SiNP nanocomposites fabricated via (c) *in situ* sol−gel and (d) solution-cast methods, at 215 K (solid blue bar), 245 K (solid green bar), and 295 K (solid orange bar).

samples are directly correlated to the lower values of D_{jump} measured for these membranes, where for example, the value of D_{jump} decreases by almost an order of magnitude when comparing 10%SiNP and 10%SiNP-SC. Again, we believe this difference is directly related to the differeinces in the silica phase formed, and thus, the final nanostructure of the Nafion-SiNP membranes fabricated via the two synthesis routes methods.

In addition to the long-range ion dynamics (i.e., D_{jump}), the local ion dynamics were also obtained from a plateau that is visible in HWHM analysis at smaller Q values, which unlike the aforementioned D_{jump}, is associated with continuous diffusion within a confined space. Please note that the Q values at which we see a plateau in HWHM may not match exactly what is expected from the EISF analysis due to poor Q resolution in the data obtained at the HFBS. The local diffusion coefficient (D_{local}) for membranes fabricated via *in situ* sol−gel and solution-cast methods, at 215 K (solid blue bars), 245 K (solid green bars), and 295 K (solid orange bars), are shown in Figures 7a,b, respectively. As expected, the value of D_{local} increased with increasing temperature for Nafion and Nafion-SiNP nanocomposites synthesized via both fabrication routes. As before, our discussion below will focus on the vanadium ion dynamics at 295 K. As seen in Figure 7a, the local diffusion coefficient decreased (to its lowest value) with thermal annealing ($(5.1 \pm 1.6) \times 10^{-6}$ cm^2 s^{-1} vs $(2.1 \pm 0.3) \times 10^{-6}$ cm^2 s^{-1} for Nafion-UA vs Nafion-A). This behavior is analogous to what was observed for the effect of thermal annealing on the jump diffusion coefficient. However, contrary to the ion dynamics behavior previously observed for long-range dynamics, the value of D_{local} is seen to increase with the introduction of SiNPs, returning to similar local ion dynamics to that of Nafion-UA. In contrast, while the local diffusion coefficient for sol−gel membranes was seen to increase with higher nanoparticle loading, the introduction of SiNPs to the solution-cast membranes resulted in a reduction in the local diffusion coefficient. ($(3.7 \pm 0.8) \times 10^{-6}$ cm^2 s^{-1} vs $(3.3 \pm 0.7) \times 10^{-6}$ cm^2 s^{-1} for Nafion-SC vs 4%SiNP-SC). The local diffusion coefficient was further reduced by almost 4-fold when the SiNP loading was increased from 4 to 10 mass %. The behavior is consistent to what was observed with that of the longer range vanadium ion dynamics (D_{jump}; see Figure 5b). Again, the difference in D_{local} with introduction of SiNP observed between *in situ* sol−gel and solution-cast membranes is probably due to the different nantostructure of these membranes.

Similar to the previous analysis, a local residence time between diffusion jumps (τ_0) can also be extracted from the HWHM data at Q_0. The values of τ_0 for *in situ* sol−gel and solution-cast membranes, at 215 K (solid blue bars), 245 K (solid green bars), and 295 K (solid orange bars), are shown in Figures 7c,d, respectively. Note that the residence time between diffusion for 10%SiNP-SC at 215 K is not shown in Figure 7d due to the large error in the measured value, which arises from the slow vanadium ion dynamics in the membrane at this low temperature. Similarly, τ_0 is seen to decrease at higher temperature while τ_0 for solution cast samples at 295 K showed an increasing trend with increased nanoparticle loading (237.3 ± 4.4 ps, 249.0 ± 10.4 ps, and 733.5 ± 39.1 ps, for Nafion-SC, 4%SiNP-SC, and 10%SiNP-SC, respectively). However, the same trend was not observed for membranes fabricated via *in situ* sol−gel process at 295 K, where a reduction in τ_0 with the introduction of SiNPs is seen (388.3 ± 18.4, 302.2 ± 9.9, and 219.1 ± 4.5 ps, for Nafion-A, 4%SiNP, and 10%SiNP, respectively). Combining D_{local} and τ_0, membranes fabricated via the *in situ* sol−gel process

https://doi.org/10.1021/acs.jpcb.4c01203
J. Phys. Chem. B 2024, 128, 5766−5780

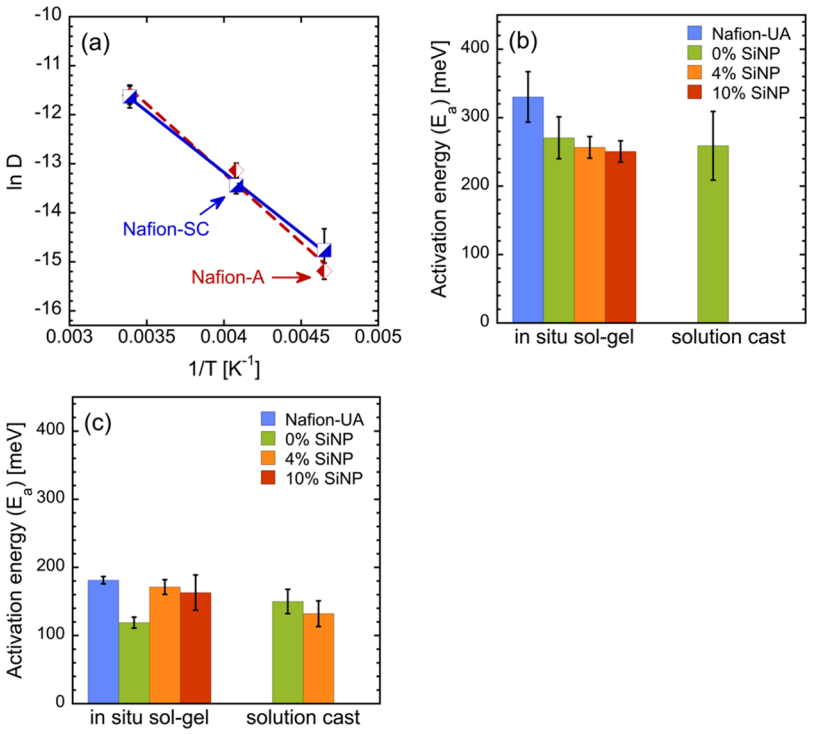

Figure 8. (a) Arrhenius plot of jump diffusion (D_{jump}) for Nafion-A (half filled red diamond) and Nafion-SC (half filled blue squares), where the dashed red line and solid blue line represent the best-fit linear regression of the data. (b) Activation energies of jump diffusion (D_{jump}) and (c) local diffusion (D_{local}) for membranes fabricated via both *in situ* sol−gel and solution-cast methods. Note that the error bars in panels (b) and (c) represent the propagated error from the best-fit linear regression of the diffusion data for each membrane.

demonstrated faster local dynamics with increasing SiNP loading, where both higher local diffusion coefficient as well as smaller local residence time were seen when SiNP content increased from 0 mass % to 4 mass % and 10 mass %. Interestingly, solution-cast membranes showed the contrary trend with the incorporation of nanoparticles, which is due to the difference in membrane nanostructure and chain flexibility with different fabrication methods.

To help the reader better understand the impact of various membrane processing routes on the dynamics of the hydrated vanadyl ion, the model parameters of some of the samples discussed above are summarized in Table 2, where the dynamic length scale (R), fraction of immobile atoms (φ), jump diffusion coefficient (D_{jump}), local diffusion coefficient (D_{local}), residence time between jump (τ), and residence time between diffusion (τ_0) for the hydrated vanadyl ion dynamics are presented. In addition, the dynamics of pure water in Nafion at room temperature, as measured from previous QENS studies, are provided in Table 2.[62,63]

Note that Nafion 117 (λ_{water} = 1), Nafion 117 (λ_{water} = 8), and Nafion 117 (λ_{water} = 16) represent water dynamics in Nafion 117 at various hydration levels (λ_{water}), where Nafion 117 (λ_{water} = 1) is the lowest hydration level and Nafion 117 (λ_{water} = 16) is fully hydrated. The level of hydration, λ_{water}, is the molar ratio of water and sulfonic acid groups of the Nafion membrane. It should also be noted that "Nafion-UA" and "Nafion 117 (λ_{water} = 16)" are equivalent membranes, as they are both Nafion 117 membranes and are both fully hydrated, allowing for a direct comparison of vanadium ion dynamics and water dynamics in Nafion. As seen from Table 2, the dynamic length scale of vanadium ion motions is larger for both *in situ* sol−gel and solution-cast ionomer nanocomposites. Further, both the residence times between jump and local motions of the hydrated vanadyl ion are significantly larger (between one and 2 orders of magnitude) when compared with that of water molecules. For example, τ and τ_0 for Nafion-UA are (41.86 ± 6.26) and (239.43 ± 4.38) ps, respectively, while those same values for the dynamics of pure water in Nafion 117 (λ_{water} = 16) are (3.6 ± 0.3) and (9.8 ± 0.7) ps, respectively.

With dynamic information as a function of temperature for both local and jump motions, the activation energies of these two motions can be ascertained, assuming Arrhenius-like behavior, from a plot of ln(D) vs T. As an example, these data for both Nafion-A and Nafion-SC are shown in Figure 8a, where the activation energies (E_a) were extracted from the slope of the best linear fitting from regression. Unfortunately, with data at only two temperatures, the values of E_a associated with jump diffusion in 4%SiNP-SC and 10%SiNP-SC are not reported in Figure 8b. Similarly, the E_a associated with local diffusion for 10%SiNP-SC is not reported in Figure 8c. Interestingly, a decrease in the E_a associated with jump diffusion (Figure 8b) was seen to decrease with the introduction of SiNPs, while the jump diffusion coefficient itself was seen to decrease by over 2-fold at 295 K for the same membranes (see solid orangle bars in Figure 5a). However, as seen in Figure 8c, the similar local diffusion coefficients observed for *in situ* sol−gel membranes correlates with the similar values of E_a associated with local diffusion for these samples. In addition, the activation energy for local diffusion is generally lower than that of jump diffusion. It is also worth noting that the activation energy for water dynamics in bulk water is approximately 180 meV,[62] which is lower than that seen for all ionomer nanocomposites in this study.

https://doi.org/10.1021/acs.jpcb.4c01203
J. Phys. Chem. B 2024, 128, 5766−5780

CONCLUSIONS

In summary, dynamics of hydrated vanadium ions in Nafion nanocomposite membranes fabricated via both an *in situ* sol−gel method and a solution-cast method were investigated using a high flux backscattering spectrometer, where vanadium ion dynamics within membranes on a molecular scale were reported for the first time. The obtained quasi-elastic scattering spectra were fit to a model that combines local diffusion within a sphere and random jump diffusion to obtain both dynamic (diffusion coefficients) and geometrical (spacial range of the dynamics) information on the observed ion motion. Interestingly, in general, both diffusion coefficients and radius that dynamics occur were seen to decrease with the introduction of SiNPs, regardless of fabrication method. In addition, reduction in vanadium ion dynamics was also observed with thermal treatment, which is a result of tuned membrane morphology and chain dynamics via annealing. These restricted dynamics of hydrated vanadium ion are in accordance with previously reported decreased vanadium ion permeability, providing a molecular level interpretation for the reduced vanadium ion crossover with thermal treatment and incorporation of silica nanoparticles, that is, the increased orderliness in polymer chain via annealing as well as the interaction between sulfonic acid groups and SiNPs can render part of the sulfonic acid groups inaccessible for vanadium ion transport, where diffusion coefficients were seen to reduce, leading to reduced crossover of vanadium ion.

ASSOCIATED CONTENT

Data Availability Statement

The data that support the findings of this study are available from the corresponding author upon reasonable request.

Supporting Information

The Supporting Information is available free of charge at https://pubs.acs.org/doi/10.1021/acs.jpcb.4c01203.

Fixed window scans (FWS), elastic incoherent structure factor (EISF), and half-width at half-maximum (HWHM) data for all Nafion−SiNP composites (PDF)

AUTHOR INFORMATION

Corresponding Author

Eric M. Davis − *Department of Chemical and Biomolecular Engineering, Clemson University, Clemson, South Carolina 29634, United States;* orcid.org/0000-0002-5633-5489; Email: ericd@clemson.edu

Authors

Xueting Wang − *Department of Chemical and Biomolecular Engineering, Clemson University, Clemson, South Carolina 29634, United States*

Apoorv Balwani − *Department of Chemical and Biomolecular Engineering, Clemson University, Clemson, South Carolina 29634, United States*

Madhusudan Tyagi − *National Institute of Standards and Technology (NIST) Center for Neutron Research (NCNR), Gaithersburg, Maryland 20899, United States; Department of Materials Science and Engineering, University of Maryland, College Park, Maryland 20742, United States*

Complete contact information is available at: https://pubs.acs.org/10.1021/acs.jpcb.4c01203

Author Contributions

X.W.: Formal analysis, Investigation, Writing − Original Draft, Visualization. A.B.: Investigation. M.T.: Formal analysis, Investigation, Writing − Review & Editing. E.M.D.: Conceptualization, Validation, Writing − Review & Editing, Supervision.

Notes

The authors declare no competing financial interest.

ACKNOWLEDGMENTS

This material is based upon work supported by the National Science Foundation under Grant No. DMR-1848347. Access to the HFBS was provided by the Center for High Resolution Neutron Scattering, a partnership between the NIST and the NSF under agreement no. DMR-2010792. Certain commercial material suppliers are identified in this paper to foster understanding. Such identification does not imply recommendation or endorsement by the NIST, nor does it imply that the materials or equipment identified are necessarily the best available for the purpose.

REFERENCES

(1) Jiang, H. R.; Sun, J.; Wei, L.; Wu, M. C.; Shyy, W.; Zhao, T. S. A High Power Density and Long Cycle Life Vanadium Redox Flow Battery. *Energy Storage Mater.* **2020**, *24*, 529−540.

(2) Lourenssen, K.; Williams, J.; Ahmadpour, F.; Clemmer, R.; Tasnim, S. Vanadium Redox Flow Batteries: A Comprehensive Review. *J. Energy Storage* **2019**, *25*, No. 100844.

(3) Huang, Z.; Mu, A.; Wu, L.; Wang, H. Vanadium Redox Flow Batteries: Flow Field Design and Flow Rate Optimization. *J. Energy Storage* **2022**, *45*, No. 103526.

(4) Li, X.; Zhang, H.; Mai, Z.; Zhang, H.; Vankelecom, I. Ion Exchange Membranes for Vanadium Redox Flow Battery (VRB) Applications. *Energy Environ. Sci.* **2011**, *4* (4), 1147.

(5) Dai, J.; Dong, Y.; Gao, P.; Ren, J.; Yu, C.; Hu, H.; Zhu, Y.; Teng, X. A Sandwiched Bipolar Membrane for All Vanadium Redox Flow Battery with High Coulombic Efficiency. *Polymer* **2018**, *140*, 233−239.

(6) Teng, X.; Yu, C.; Wu, X.; Dong, Y.; Gao, P.; Hu, H.; Zhu, Y.; Dai, J. PTFE/SPEEK/PDDA/PSS Composite Membrane for Vanadium Redox Flow Battery Application. *J. Mater. Sci.* **2018**, *53* (7), 5204−5215.

(7) Jung, H.-Y.; Cho, M.-S.; Sadhasivam, T.; Kim, J.-Y.; Roh, S.-H.; Kwon, Y. High Ionic Selectivity of Low Permeable Organic Composite Membrane with Amphiphilic Polymer for Vanadium Redox Flow Batteries. *Solid State Ion.* **2018**, *324*, 69−76.

(8) Wang, G.; Zhang, J.; Zhang, J.; Chen, J.; Zhu, S.; Liu, X.; Wang, R. Sulfonated Poly(Ether Ether Ketone)/Poly(Vinylidene Fluoride)/Graphene Composite Membrane for a Vanadium Redox Flow Battery. *J. Solid State Electrochem.* **2017**, *21* (4), 1185−1194.

(9) Ye, J.; Yuan, D.; Ding, M.; Long, Y.; Long, T.; Sun, L.; Jia, C. A Cost-Effective Nafion/Lignin Composite Membrane with Low Vanadium Ion Permeation for High Performance Vanadium Redox Flow Battery. *J. Power Sources* **2021**, *482*, No. 229023.

(10) Domhoff, A.; Balwani, A.; Martin, T. B.; Davis, E. M. Leveraging Nanoparticle Dispersion State To Tune Vanadium Ion Selectivity of Nanophase-Segregated Ionomer Nanocomposites for Redox Flow Batteries. *ACS Appl. Energy Mater.* **2019**, *2* (12), 8535−8549.

(11) Domhoff, A.; Martin, T. B.; Silva, M. S.; Saberi, M.; Creager, S.; Davis, E. M. Enhanced Proton Selectivity in Ionomer Nanocomposites Containing Hydrophobically Functionalized Silica Nanoparticles. *Macromolecules* **2021**, *54* (1), 440−449.

(12) Balwani, A.; Faraone, A.; Davis, E. M. Impact of Nanoparticles on the Segmental and Swelling Dynamics of Ionomer Nanocomposite Membranes. *Macromolecules* **2019**, *52* (5), 2120−2130.

(13) Xi, J.; Wu, Z.; Qiu, X.; Chen, L. Nafion/SiO2 Hybrid Membrane for Vanadium Redox Flow Battery. *J. Power Sources* **2007**, *166* (2), 531−536.
(14) Jiang, R.; Kunz, H. R.; Fenton, J. M. Composite Silica/Nafion® Membranes Prepared by Tetraethylorthosilicate Sol−Gel Reaction and Solution Casting for Direct Methanol Fuel Cells. *J. Membr. Sci.* **2006**, *272* (1−2), 116−124.
(15) Mauritz, K. A.; Warren, R. M. Microstructural Evolution of a Silicon Oxide Phase in a Perfluorosulfonic Acid Ionomer by an in Situ Sol-Gel Reaction. 1. Infrared Spectroscopic Studies. *Macromolecules* **1989**, *22* (4), 1730−1734.
(16) Miyake, N.; Wainright, J. S.; Savinell, R. F. Evaluation of a Sol-Gel Derived Nafion/Silica Hybrid Membrane for Proton Electrolyte Membrane Fuel Cell Applications: I. Proton Conductivity and Water Content. *J. Electrochem. Soc.* **2001**, *148* (8), A898.
(17) Deng, Q.; Moore, R. B.; Mauritz, K. A. Nafion®/(SiO2, ORMOSIL, and Dimethylsiloxane) Hybrids Viain Situ Sol-Gel Reactions: Characterization of Fundamental Properties. *J. Appl. Polym. Sci.* **1998**, *68* (5), 747−763.
(18) Ghassemzadeh, L.; Pace, G.; Di Noto, V.; Müller, K. Effect of SiO2 on the Dynamics of Proton Conducting [Nafion/(SiO2)X] Composite Membranes: A Solid-State 19F NMR Study. *Phys. Chem. Chem. Phys.* **2011**, *13* (20), 9327.
(19) Aricò, A. S.; Baglio, V.; Antonucci, V.; Nicotera, I.; Oliviero, C.; Coppola, L.; Antonucci, P. L. An NMR and SAXS Investigation of DMFC Composite Recast Nafion Membranes Containing Ceramic Fillers. *J. Membr. Sci.* **2006**, *270* (1−2), 221−227.
(20) Davis, E. M.; Kim, J.; Oleshko, V. P.; Page, K. A.; Soles, C. L. Uncovering the Structure of Nafion-SiO $_2$ Hybrid Ionomer Membranes for Prospective Large-Scale Energy Storage Devices. *Adv. Funct. Mater.* **2015**, *25* (26), 4064−4075.
(21) Yin, C.; Wang, Z.; Luo, Y.; Li, J.; Zhou, Y.; Zhang, X.; Zhang, H.; Fang, P.; He, C. Thermal Annealing on Free Volumes, Crystallinity and Proton Conductivity of Nafion Membranes. *J. Phys. Chem. Solids* **2018**, *120*, 71−78.
(22) Page, K. A.; Cable, K. M.; Moore, R. B. Molecular Origins of the Thermal Transitions and Dynamic Mechanical Relaxations in Perfluorosulfonate Ionomers. *Macromolecules* **2005**, *38* (15), 6472−6484.
(23) Hallinan, D. T.; Elabd, Y. A. Diffusion and Sorption of Methanol and Water in Nafion Using Time-Resolved Fourier Transform Infrared−Attenuated Total Reflectance Spectroscopy. *J. Phys. Chem. B* **2007**, *111* (46), 13221−13230.
(24) Hallinan, D. T.; Elabd, Y. A. Diffusion of Water in Nafion Using Time-Resolved Fourier Transform Infrared−Attenuated Total Reflectance Spectroscopy. *J. Phys. Chem. B* **2009**, *113* (13), 4257−4266.
(25) Naik, A. N.; Agarwal, C.; Chaudhury, S.; Goswami, A. Non-Stationary Radiotracer Method for Diffusion Coefficients of Cs^{+}, Ba^{2+}, Eu^{3+} Tracers in Nafion-117 Membrane. *Sep. Sci. Technol.* **2017**, *52* (14), 2379−2384.
(26) Goswami, A.; Acharya, A.; Pandey, A. K. Study of Self-Diffusion of Monovalent and Divalent Cations in Nafion-117 Ion-Exchange Membrane. *J. Phys. Chem. B* **2001**, *105* (38), 9196−9201.
(27) Pourcelly, G.; Sistat, P.; Chapotot, A.; Gavach, C.; Nikonenko, V. Self diffusion and conductivity in NafionR membranes in contact with NaCl+CaCl2 solutions. *J. Membr. Sci.* **1996**, *110*, 69−78.
(28) Gong, X.; Bandis, A.; Tao, A.; Meresi, G.; Wang, Y.; Ingle, P. T. *Self-Diffusion of Water, Ethanol and Decāuropentane in Pēruorosulfonate Ionomer by Pulse ®eld Gradient NMR*. 2001.
(29) Jayakody, J. R. P.; Stallworth, P. E.; Mananga, E. S.; Farrington-Zapata, J.; Greenbaum, S. G. High Pressure NMR Study of Water Self-Diffusion in NAFION-117 Membrane. *J. Phys. Chem. B* **2004**, *108* (14), 4260−4262.
(30) Giotto, M. V.; Zhang, J.; Inglefield, P. T.; Wen; Jones, A. A. Nanophase Structure and Diffusion in Swollen Perfluorosulfonate Ionomer: An NMR Approach. *Macromolecules* **2003**, *36* (12), 4397−4403.
(31) Volino, F.; Pineri, M.; Dianoux, A. J.; De Geyer, A. Water Mobility in a Water-Soaked Nafion® Membrane: A High-Resolution Neutron Quasielastic Study. *J. Polym. Sci. Polym. Phys. Ed.* **1982**, *20* (3), 481−496.
(32) Perrin, J.-C.; Lyonnard, S.; Volino, F.; Guillermo, A. Gaussian Model for Localized Translational Motion. Application to Water Dynamics in Nafion® Studied by Quasi-Elastic Neutron Scattering. *Eur. Phys. J. Spec. Top.* **2007**, *141* (1), 57−60.
(33) Perrin, J.-C.; Lyonnard, S.; Volino, F. Quasielastic Neutron Scattering Study of Water Dynamics in Hydrated Nafion Membranes. *J. Phys. Chem. C* **2007**, *111* (8), 3393−3404.
(34) Pivovar, A. M.; Pivovar, B. S. Dynamic Behavior of Water within a Polymer Electrolyte Fuel Cell Membrane at Low Hydration Levels. *J. Phys. Chem. B* **2005**, *109* (2), 785−793.
(35) Volino, F.; Dianoux, A. J. Neutron Incoherent Scattering Law for Diffusion in a Potential of Spherical Symmetry: General Formalism and Application to Diffusion inside a Sphere. *Mol. Phys.* **1980**, *41* (2), 271−279.
(36) Paciaroni, A.; Casciola, M.; Cornicchi, E.; Marconi, M.; Onori, G.; Pica, M.; Narducci, R. Temperature-Dependent Dynamics of Water Confined in Nafion Membranes. *J. Phys. Chem. B* **2006**, *110* (28), 13769−13776.
(37) Doster, W.; Diehl, M.; Gebhardt, R.; Lechner, R. E.; Pieper, J. TOF-Elastic Resolution Spectroscopy: Time Domain Analysis of Weakly Scattering (Biological) Samples. *Chem. Phys.* **2003**, *292* (2−3), 487−494.
(38) Kruteva, M. Dynamics Studied by Quasielastic Neutron Scattering (QENS). *Adsorption* **2021**, *27* (5), 875−889.
(39) Hickner, M. A. Water-Mediated Transport in Ion-Containing Polymers. *J. Polym. Sci., Part B: Polym. Phys.* **2012**, *50* (1), 9−20.
(40) Pivovar, A. M.; Pivovar, B. S. Dynamic Behavior of Water within a Polymer Electrolyte Fuel Cell Membrane at Low Hydration Levels. *J. Phys. Chem. B* **2005**, *109* (2), 785−793.
(41) Page, K. A.; Park, J. K.; Moore, R. B.; Garcia Sakai, V. Direct Analysis of the Ion-Hopping Process Associated with the α-Relaxation in Perfluorosulfonate Ionomers Using Quasielastic Neutron Scattering. *Macromolecules* **2009**, *42* (7), 2729−2736.
(42) Magazù, S.; Migliardo, F.; Benedetto, A. Mean Square Displacements from Elastic Incoherent Neutron Scattering Evaluated by Spectrometers Working with Different Energy Resolution on Dry and Hydrated (H_2O and D_2O) Lysozyme. *J. Phys. Chem. B* **2010**, *114* (28), 9268−9274.
(43) Roosen-Runge, F.; Seydel, T. A Generalized Mean-Squared Displacement from Inelastic Fixed Window Scans of Incoherent Neutron Scattering as a Model-Free Indicator of Anomalous Diffusion Confinement. *EPJ. Web Conf.* **2015**, *83*, 02015.
(44) Hirata, F. On the Interpretation of the Temperature Dependence of the Mean Square Displacement (MSD) of Protein, Obtained from the Incoherent Neutron Scattering. *J. Mol. Liq.* **2018**, *270*, 218−226.
(45) Ballhausen, C. J.; Gray, H. B. The Electronic Structure of the Vanadyl Ion. *Inorg. Chem.* **1962**, *1* (1), 111−122.
(46) Reuben, J.; Fiat, D. Magnetic Resonance Studies of Ion Solvation. The Hydration of the Vanadyl(IV) Ion. *Inorg. Chem.* **1967**, *6* (3), 579−583.
(47) Vijayakumar, M.; Burton, S. D.; Huang, C.; Li, L.; Yang, Z.; Graff, G. L.; Liu, J.; Hu, J.; Skyllas-Kazacos, M. Nuclear Magnetic Resonance Studies on Vanadium(IV) Electrolyte Solutions for Vanadium Redox Flow Battery. *J. Power Sources* **2010**, *195* (22), 7709−7717.
(48) Soles, C. L.; Burns, A. B.; Ito, K.; Chan, E. P.; Douglas, J. F.; Wu, J.; Yee, A. F.; Shih, Y.-T.; Huang, L.; Dimeo, R. M.; Tyagi, M. Why Enhanced Subnanosecond Relaxations Are Important for Toughness in Polymer Glasses. *Macromolecules* **2021**, *54* (5), 2518−2528.
(49) Balwani, A.; Faraone, A.; Davis, E. M. Impact of Nanoparticles on the Segmental and Swelling Dynamics of Ionomer Nanocomposite Membranes. *Macromolecules* **2019**, *52* (5), 2120−2130.

https://doi.org/10.1021/acs.jpcb.4c01203
J. Phys. Chem. B 2024, 128, 5766−5780

(50) Kusoglu, A.; Weber, A. Z. New Insights into Perfluorinated Sulfonic-Acid Ionomers. *Chem. Rev.* **2017**, *117* (3), 987−1104.
(51) Domhoff, A.; Wang, X.; Silva, M. S.; Creager, S.; Martin, T. B.; Davis, E. M. Role of Nanoparticle Size and Surface Chemistry on Ion Transport and Nanostructure of Perfluorosulfonic Acid Ionomer Nanocomposites. *Soft Matter* **2022**, *18*, 3342 DOI: 10.1039/D1SM01573G.
(52) Kusoglu, A.; Kushner, D.; Paul, D. K.; Karan, K.; Hickner, M. A.; Weber, A. Z. Impact of Substrate and Processing on Confinement of Nafion Thin Films. *Adv. Funct Mater.* **2014**, *12*, 4763 DOI: 10.1002/adfm.201304311.
(53) Schwenzer, B.; Zhang, J.; Kim, S.; Li, L.; Liu, J.; Yang, Z. Membrane Development for Vanadium Redox Flow Batteries. *ChemSusChem* **2011**, *4* (10), 1388−1406.
(54) Schwenzer, B.; Kim, S.; Vijayakumar, M.; Yang, Z.; Liu, J. Correlation of Structural Differences between Nafion/Polyaniline and Nafion/Polypyrrole Composite Membranes and Observed Transport Properties. *J. Membr. Sci.* **2011**, *372* (1−2), 11−19.
(55) Okada, T.; Satou, H.; Okuno, M.; Yuasa, M. Ion and Water Transport Characteristics of Perfluorosulfonated Ionomer Membranes with H^+ and Alkali Metal Cations. *J. Phys. Chem. B* **2002**, *106* (6), 1267−1273.
(56) Okada, T.; Ayato, Y.; Yuasa, M.; Sekine, I. The Effect of Impurity Cations on the Transport Characteristics of Perfluorosulfonated Ionomer Membranes. *J. Phys. Chem. B* **1999**, *103* (17), 3315−3322.
(57) Steck, A.; Yeager, H. L. Water Sorption and Cation-Exchange Selectivity of a Perfluorosulfonate Ion-Exchange Polymer. *Anal. Chem.* **1980**, *52* (8), 1215−1218.
(58) Tandon, R.; Pintauro, P. N. Divalent/Monovalent Cation Uptake Selectivity in a Nation Cation-Exchange Membrane: Experimental and Modeling Studies. *J. Membr. Sci.* **1997**, *136*, 207 DOI: 10.1016/S0376-7388(97)00167-1.
(59) Bontha', J. R.; Pintauro, P. N. *A NAFION CATION EXCHANGE MEMBRANE*.
(60) Vijayakumar, M.; Bhuvaneswari, M. S.; Nachimuthu, P.; Schwenzer, B.; Kim, S.; Yang, Z.; Liu, J.; Graff, G. L.; Thevuthasan, S.; Hu, J. Spectroscopic Investigations of the Fouling Process on Nafion Membranes in Vanadium Redox Flow Batteries. *J. Membr. Sci.* **2011**, *366* (1−2), 325−334.
(61) KOMOROSKI, R. A.; MAURITZ, K. A. Nuclear Magnetic Resonance Studies and the Theory of Ion Pairing in Perfluorosulfonate Ionomers. *ACS Symposium Series* 1982, *Vol. 180*, DOI: DOI: 10.1021/bk-1982-0180.ch007.
(62) Melchior, J.-P.; Jalarvo, N. H. A Quasielastic Neutron Scattering Study of Water Diffusion in Model Anion Exchange Membranes over Localized and Extended Volume Increments. *J. Phys. Chem. C* **2019**, *123* (23), 14195−14206.
(63) Osti, N. C.; Coté, A.; Mamontov, E.; Ramirez-Cuesta, A.; Wesolowski, D. J.; Diallo, S. O. Characteristic Features of Water Dynamics in Restricted Geometries Investigated with Quasi-Elastic Neutron Scattering. *Chem. Phys.* **2016**, *465−466*, 1−8.
(64) Cavatorta, F.; Deriu, A.; Cola, D. D.; Middendorf, H. D. Diffusive Properties of Water Studied by Incoherent Quasi-Elastic Neutron Scattering. *J. Phys.: Condens. Matter* **1994**, *6* (23A), A113−A117.
(65) Teixeira, J.; Bellissent-Funel, M.-C.; Chen, S. H.; Dianoux, A. J. Experimental Determination of the Nature of Diffusive Motions of Water Molecules at Low Temperatures. *Phys. Rev. A* **1985**, *31* (3), 1913−1917.

https://doi.org/10.1021/acs.jpcb.4c01203
J. Phys. Chem. B 2024, 128, 5766−5780